3rd International Symposium
"Geodesy and Physics of the Earth"

DDR Weimar, Oct. 25 - 31, 1976

NEW RESULTS CONCERNING THE GEOMAGNETIC EFFECT IN THE UPPER ATMOSPHERE

I. Almár, A. Horváth, E. Illés-Almár
/Hungary/

ABSTRACT. 89 equivalent duration values based on more than 30 000 satellite observations were used to derive relations between different geomagnetic parameters and the correlated changes in upper atmospheric density during magnetospheric storms. The results demonstrate how the storm-time relative density increase depends on the intensity of the magnetospheric storm, on the altitude of the perigee and on its geocentric distance from the center of the diurnal bulge.

РЕЗЮМЕ: НОВЫЕ РЕЗУЛЬТАТЫ ИССЛЕДОВАНИЯ ГЕОМАГНИТНОГО ЭФФЕКТА ВЕРХНЕЙ АТМОСФЕРЫ

И.Алмар, А.Хорват, Е.Иллеш-Алмар (Венгрия)

На основе более 30 000 наблюдений ИСЗ были определены 89 значений эквивалентных продолжительностей для того, чтобы выводить отношения между разными геомагнитными параметрами и соответствующими им изменениями плотности верхней атмосферы во время магнитосферных бурь. Результаты показывают как зависит относительное увеличение плотности во время бури от интенсивности магнитосферной бури, от высоты перигея и от геоцентрического расстояния от центра суточного горба.

Introduction

We proposed in 1970 to use the integral of the relative density variation curve as a new parameter to characterize the total intensity of the atmospheric response during large magnetospheric storms[1]. Succesively 89 "equivalent duration" /D/ parameters have been derived mainly using three sources: 1/ optical observations of artificial satellites in order to determine the D value by our PERLO - SPACECOOR method [2] , 2/ orbital elements from the GSFC and other computing centers, 3/ some $\dot{P}$ or ρ curves /published in the literature/ having a sufficient resolution in time.

All data concerning the observational material in question are summarized in Table I.

Table 1

time interval:	1960-1972
number of geomagnetic storms:	22
number of different satellites:	34
number of equivalent durations:	89
number of independent determinations:	125
number of observations used:	~ 30 000
height interval:	200 - 1200 km

The observed equivalent duration values /D_{obs}/ have been directly compared with similar ones, obtained by means of direct integration of the corresponding ρ curves of the Jacchia-71 model /D_{J71}/. As we already emphasized in earlier papers [3, 4] , below 300 km the total response is significantly more intensive than supposed by Jacchia /Fig. 1/. A least squares solution has been fit to the whole interval transformed from the linear relation between log $\frac{D_{obs}}{D_{J71}}$ and log /h_{ref} - 200/ as demonstrated on Fig. 2. The correlation is, however, rather poor $/r^2 = 0.45/$ pointing to the need of a more comprehensive investigation in order to determine how the storm-time relative density increase depends on different geometric and physical parameters.

Results

As it was already suggested [5] , D values coming from different magnetospheric storms should be reduced to unit storm intensity before analysing their dependence on height, latitude, $S_{10.7}$ etc. The connection between storm intensity and changes in solar wind energy /directly influencing the magnetosphere/, is at present not available, therefore only secondary parameters, like a_p, K_p can be used. There are several empirical formulae in different models giving a direct connection between a function of a geomagnetic index and the corresponding relative density change in the upper atmosphere. Integrating both sides from the beginning till the end of the strom the equivalent duration is devided into two components:

the β function representing its dependence on invariable parameters during the storm $/h_{ref}$, φ etc/;

the L function, the integral of an arbitrary geomagnetic index, representing its dependence on storm intensity.

The β value is therefore the equivalent duration reduced to unit total storm intensity.

Five slightly different L definitions have been introduced, corresponding to five possible model connections:

$$L_1 = \int_{t_1}^{t_2} \ln \frac{a_p}{a_{p_0}} dt; \qquad L_2 = \int_{t_1}^{t_2} (a_p - a_{p_0}) dt$$

$$L_3 = \int_{t_1}^{t_2} \frac{a_p - a_{p_0}}{a_{p_0}} dt; \qquad L_4 = \int_{t_1}^{t_2} a_p dt; \qquad L_5 = \int_{t_1}^{t_2} (K_p - K_{p_0}) dt$$

The dependence of all β_i^{obs} values - reduced from the observed equivalent durations by means of the five different L definitions - have been thoroughly investigated on the following parameters: L, log ρ_0, φ, φ_{geom}, Ψ_{sun}, LST, $\bar{S}_{10.7}$, h_{ref}, Ψ_B. No remaining dependence has been found on L. From those parameters, characterizing the spatial position of the point in question, the altitude /h_{ref}/ and - somewhat arbitrarily - the angular distance from the center of the diurnal bulge /Ψ_B/ have been selected. /Other parameters are less sensitive./

Fig. 3 and 4 demonstrate how β_i depend on h_{ref} and Ψ_B. There is an obvious increase with height from 200 to 800 km /Fig. 3/ and a more complex dependence on Ψ_B varying with altitude /Fig. 4/. Several model relations are also plotted for comparison. Roemer [6], for instance, derived a constant β_2 function, which is obviously not correct. In another model β_4 is a linear function of height only [7]. In the atmospheric model of the Space Research Institute of the Soviet Union [8] β_1 is a linear function of height and $S_{10.7}$. These model relations can be considered as a first approximation only. It is more difficult to have a direct comparison with the Jacchia-71 model [9], which does not contain any explicit relation between density and a geomagnetic index; therefore another approach was used.

First of all it has been analysed whether the selection of L effects in this way or another significantly our conclusions. ~~Second~~ Third order ~~surfaces~~ polynomials with independent variables h_{ref} and Ψ_B have been fitted to all β_1 ... β_5 values separately. The functions contain 10 independent coefficients: $a_1 \ldots a_{10}$. After a normalisation procedure the five equations have similar coefficients demonstrating that all definitions are almost equally suitable. The parameter characterizing the scatter of the points around tho surface proved to be smallest at β_2, therefore this definition has been considered optimal.

The β_2 surface shows clearly the complex dependence of the atmospheric reaction on height and position /Fig. 5/. The total density change is strongest in the bulge at low altitudes, but has another maximum at higher altitudes around $\Psi_B = 90^o$. The same surface has been constructed from calculated β_{J71} values and plotted for comparison with the Jacchia-71 model. The difference between the observed and the model surface is important along the h_{ref} axis. Comparing directly the corresponding coefficients in the two equations we came to the same conclusion. If the number of free coefficients of the solution is reduced from 10 to 7 by making 3 badly determined coefficients equal zero, the significance of all other coefficients is considerably improved. The new coefficients are similar /within error limit/ in the equations of the observed and model surfaces respectively - except terms containing h and h^3. It can be pointed out that the Jacchia model correctly describes the variability with Ψ_B but overestimates the height dependence. Fig. 6 finally demonstrates the dependence of β_2 on h_{ref} and Ψ_B in another way. The observed β_2 values are plotted in different /h_{ref}, Ψ_B/ intervals and confronted by curves derived from our model equation for the interval in question.

Conclusions

By means of 89 equivalent duration values it has been demonstrated that all earlier model relations between geomagnetic indices and corresponding changes in upper atmospheric density should be modified during strong geomagnetic storms. The relative density increase is proportional to a suitably selected geomagnetic index and its dependence on spatial position can be described from 200 to 1200 km as follows: /Fig. 7/

$$\beta_2^{obs} = 8{,}20.\ 10^{-3} + 2{,}24.10^{-5}\ \bar{h} + 2{,}99.10^{-5}\ \bar{\Psi}_B + 1{,}75.10^{-7}\ \bar{h}\bar{\Psi}_B - 3{,}91.10^{-11}\ \bar{h}^3 - 3{,}92.10^{-10}\ \bar{h}^2\bar{\Psi}_B - 1{,}78.10^{-9}\ \bar{h}\bar{\Psi}_B^2$$

$$\bar{h} = h - 200 \qquad \bar{\Psi}_B = \Psi_B - 90^\circ$$

R e f e r e n c e s

[1] I. Almár, E. Illés-Almár, Space Research XI. Berlin /1971/

[2] A. Horváth, E. Illés-Almár, Nabliudenia ISZ No.14 Bucharest /1974/

[3] I. Almár, Nabliudenia ISZ No.14 Bucharest /1974/

[4] I. Almár, E. Illés-Almár, Space Research XIII. Berlin /1973/

[5] I. Almár, E. Illés-Almár, A. Horváth, Paper presented at the XVIIIth COSPAR Plenary Meeting, Varna 1975

[6] M. Roemer, Veröffentlichungen der Astr. Institute Bonn No.85 /1972/

[7] Handbook of Geophysics and Space Environment 3.6.2.

[8] P. E. Elyasberg, Prikladnüe zadachi kosmicheskoj ballistiki, Nauka /1973/

[9] L.G. Jacchia, SAO Special Report 332 /1971/

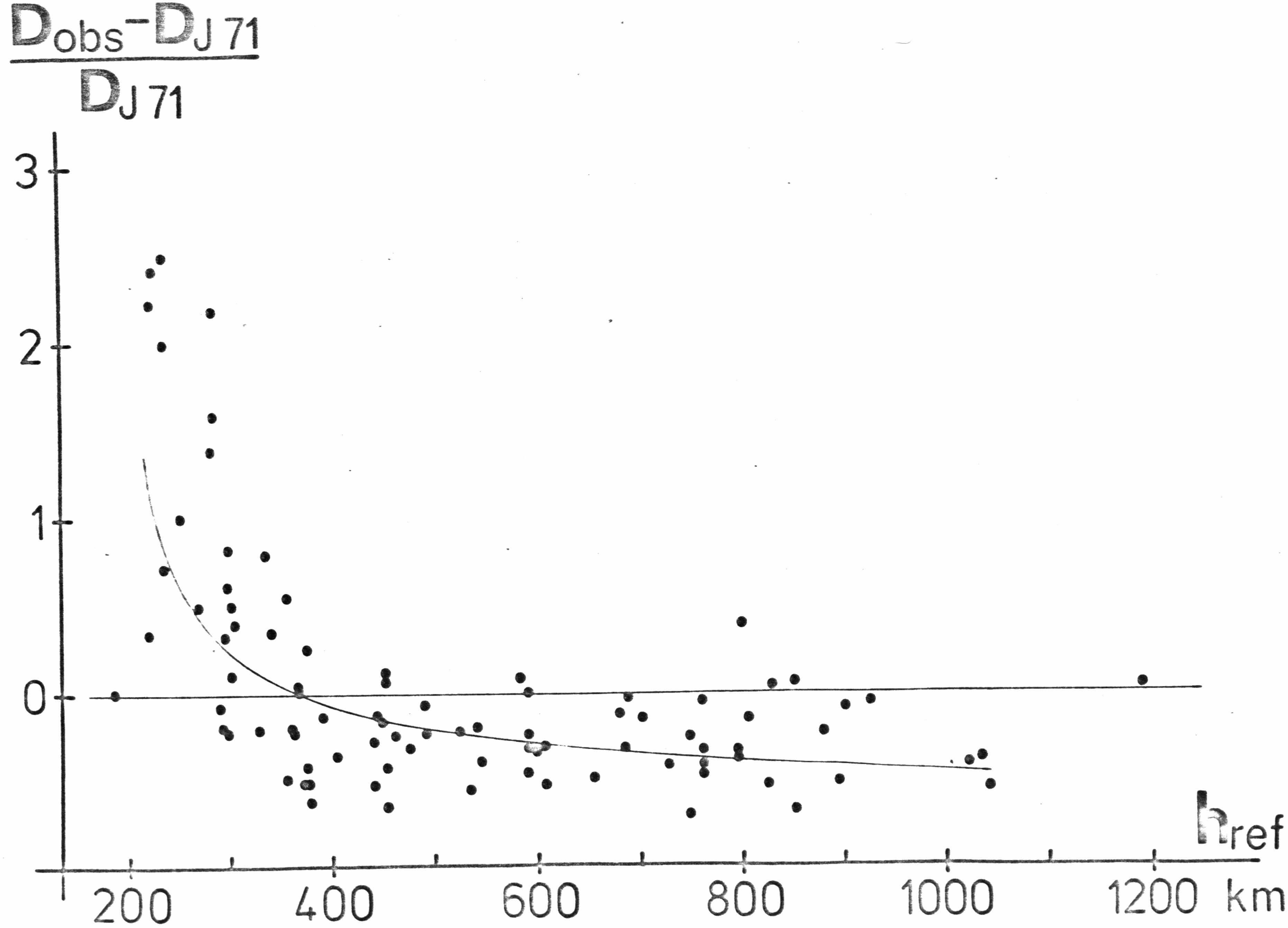

Fig. 1

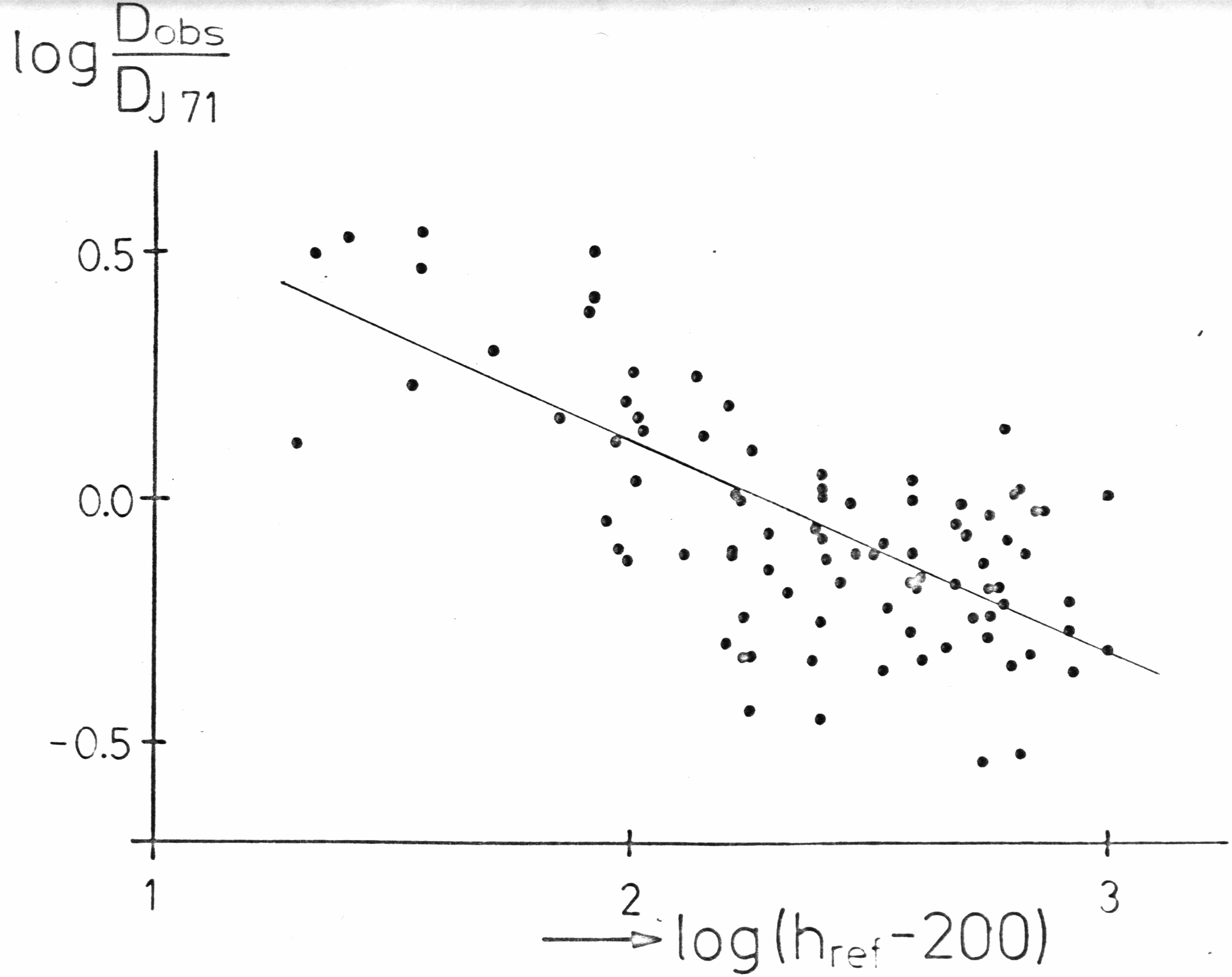

Fig. 2.

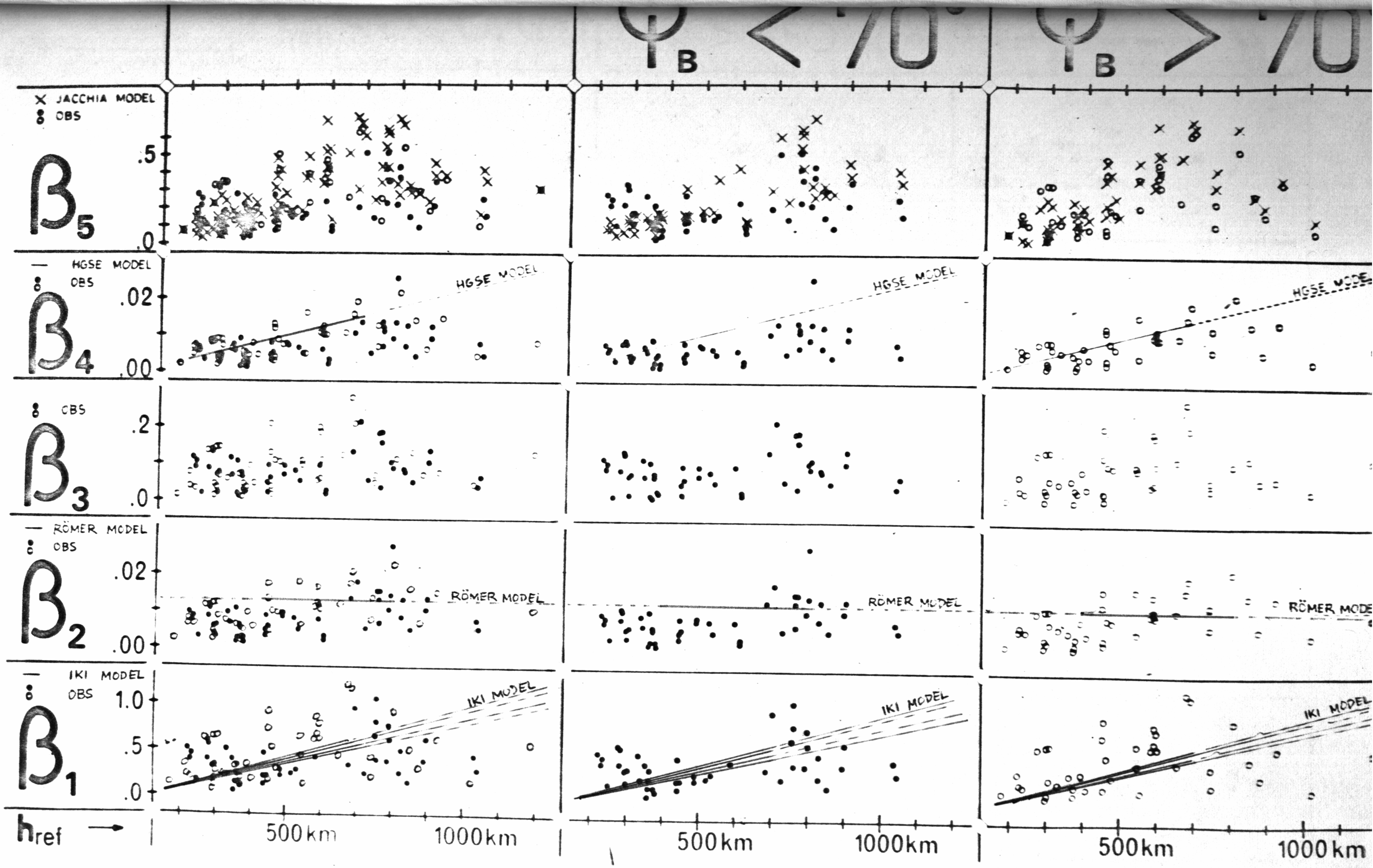

$\Psi_B < 70°$
$\Psi_B > 70°$
× JACCHIA MODEL
OBS
β_5
.5
.0
— HGSE MODEL
OBS
β_4
.02
.00
HGSE MODEL
OBS
β_3
.2
.0
— RÖMER MODEL
OBS
β_2
.02
.00
RÖMER MODEL
— IKI MODEL
OBS
β_1
1.0
.5
.0
IKI MODEL
h_{ref} →
500km
1000km

Fig. 3

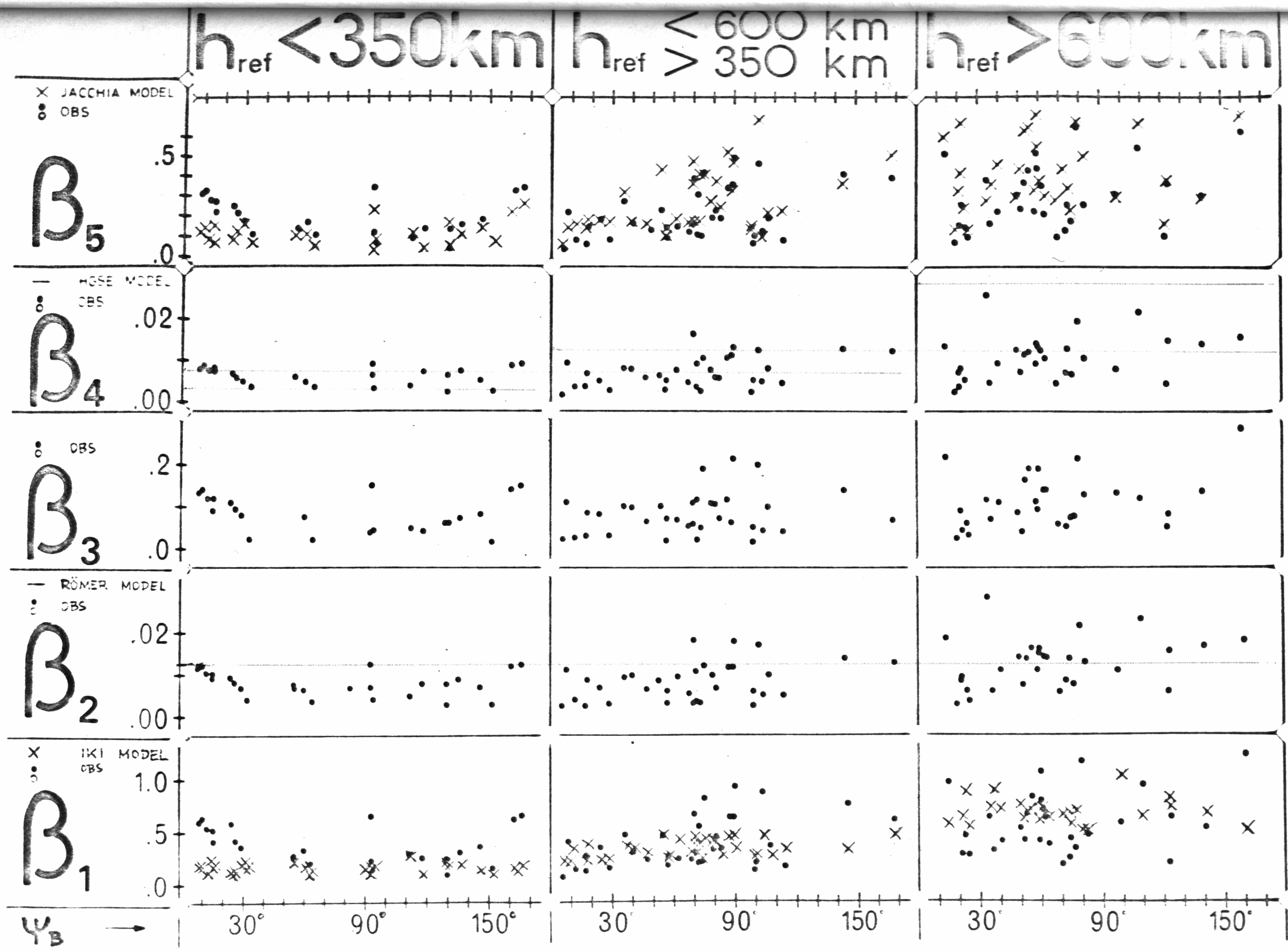

h_ref < 350 km
h_ref < 600 km
h_ref > 350 km
h_ref > 600 km
× JACCHIA MODEL
OBS
β5
.5
.0
— HOSE MODEL
OBS
β4
.02
.00
OBS
β3
.2
.0
— RÖMER MODEL
OBS
β2
.02
.00
× IKI MODEL
OBS
β1
1.0
.5
.0
Ψ_B →
30°
90°
150°

Fig. 4.

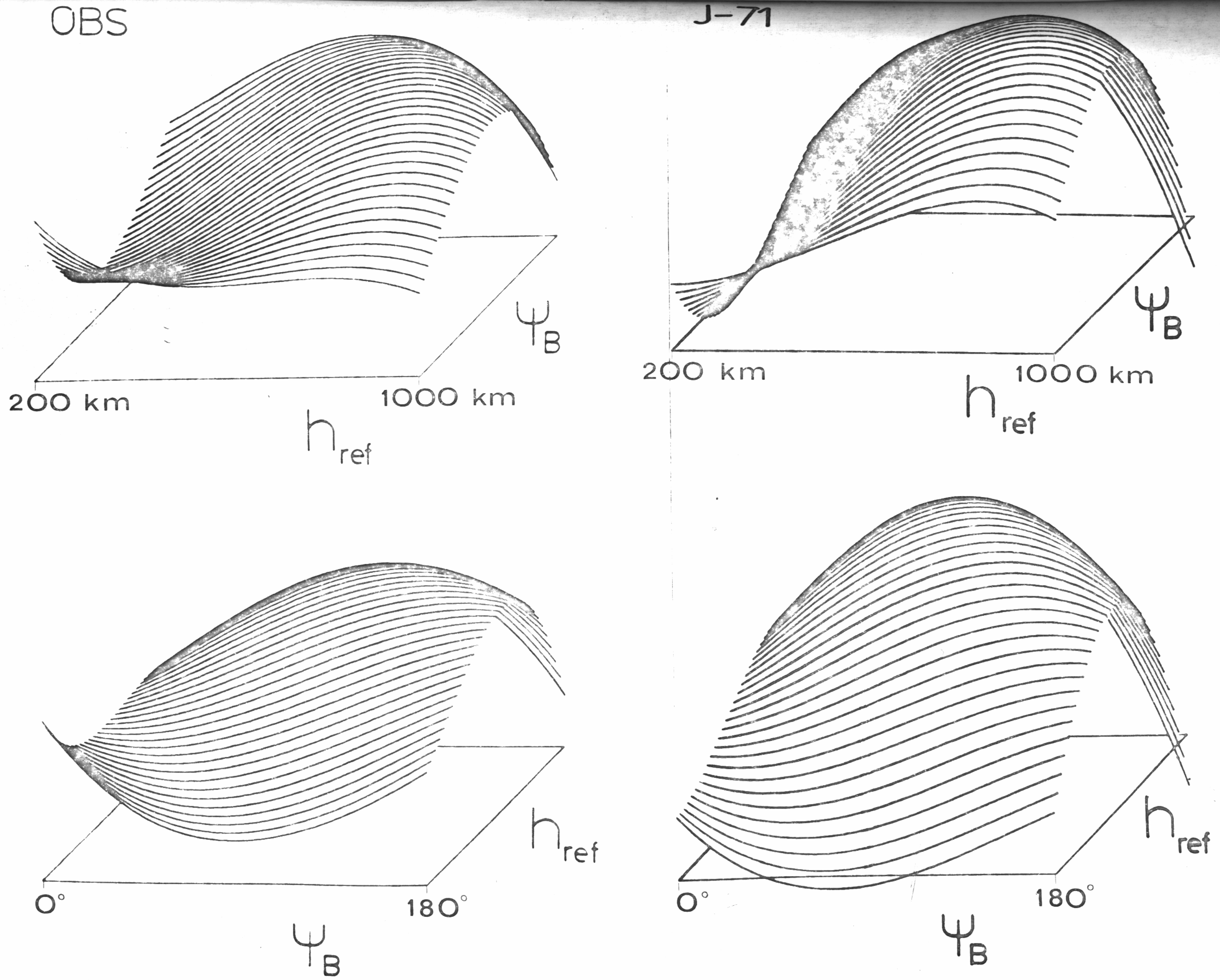

Fig. 5

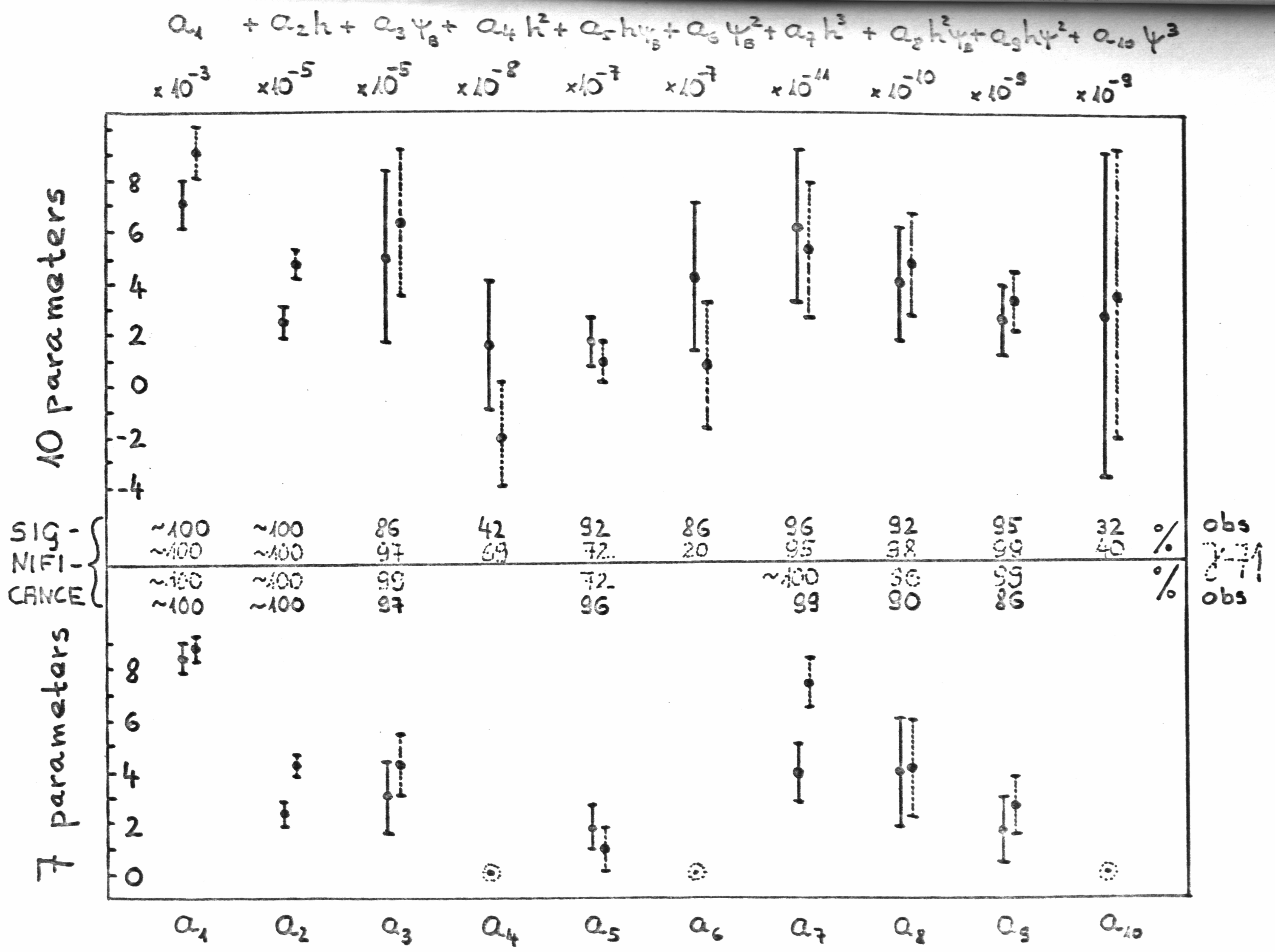

a1 + a2 h + a3 ψB + a4 h² + a5 hψB + a6 ψB² + a7 h³ + a8 h²ψB + a9 hψ² + a10 ψ³
x 10⁻³ x 10⁻⁵ x 10⁻⁵ x 10⁻⁸ x 10⁻⁷ x 10⁻⁷ x 10⁻¹¹ x 10⁻¹⁰ x 10⁻⁹ x 10⁻⁹
10 parameters
SIG-NIFI-CANCE
7 parameters
~100 ~100 86 42 92 86 96 92 95 32 % obs
~100 ~100 97 69 72 20 95 98 99 40
~100 ~100 99 72 ~100 96 99 %
~100 ~100 97 96 99 90 86 obs
a1 a2 a3 a4 a5 a6 a7 a8 a9 a10

Fig. 5 c

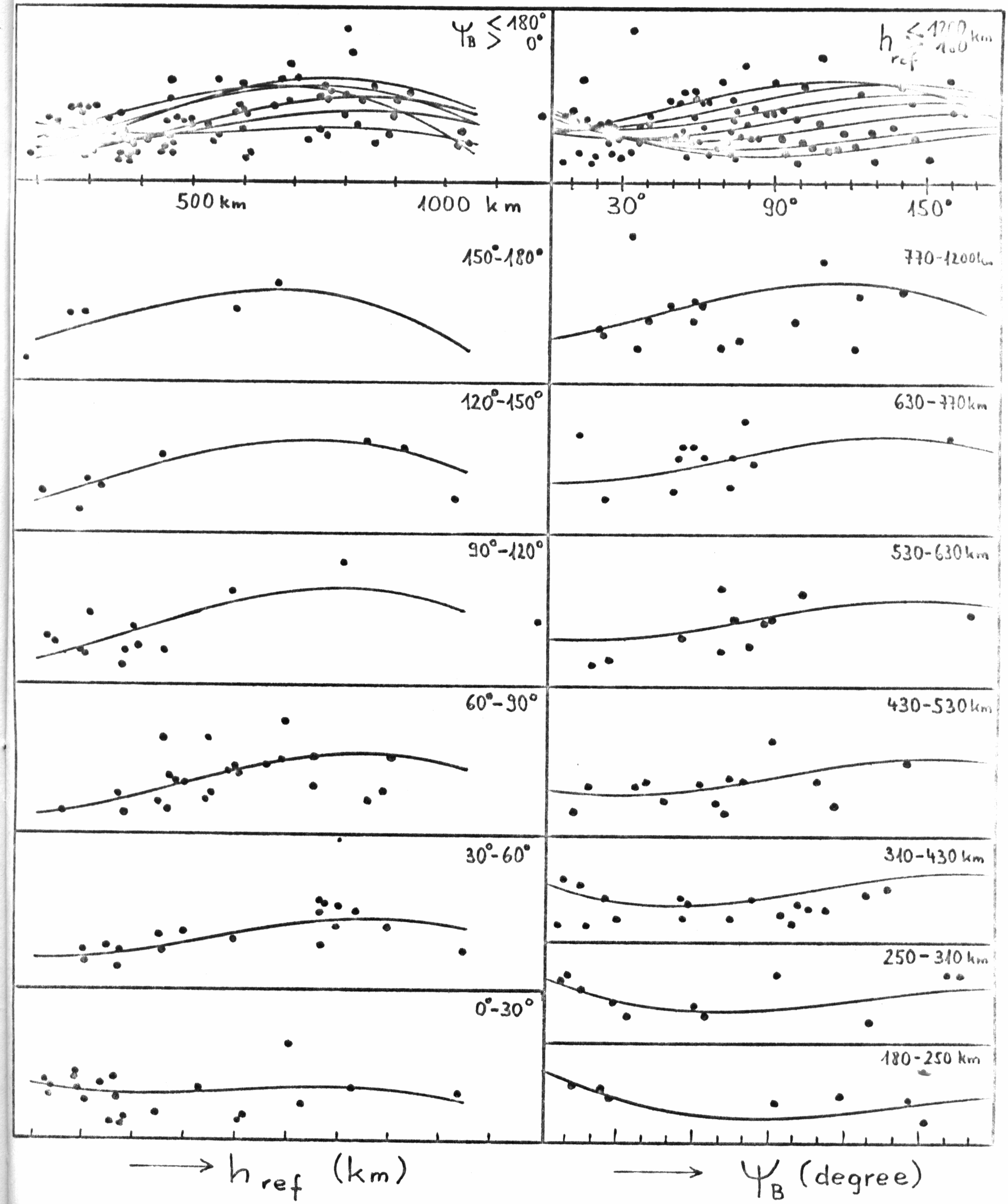

Ψ_B ≤ 180° ≥ 0°
500 km
1000 km
150°-180°
120°-150°
90°-120°
60°-90°
30°-60°
0°-30°
h_ref (km)
30°
90°
150°
770-1200 km
630-770 km
530-630 km
430-530 km
310-430 km
250-310 km
180-250 km
Ψ_B (degree)

Fig 6

$$
\rho = \begin{cases} \rho_0 + \rho_0 \beta_1 \ln \dfrac{a_p}{a_{p_0}} \\ \rho_0 + \rho_0 \beta_2 (a_p - a_{p_0}) \\ \rho_0 + \rho_0 \beta_3 \dfrac{a_p - a_{p_0}}{a_{p_0}} \\ \rho_0 + \rho_0 \beta_4 \, a_p \\ \rho_0 + \rho_0 \beta_5 (K_p - K_{p_0}) \end{cases}
$$

$$
\beta_i = a_1 + a_2(h-200) + a_3(\psi_B - 90) + a_5(h-200)(\psi_B - 90) + a_7(h-200)^3 + a_8(h-200)^2(\psi_B - 90) + a_9(h-200)(\psi_B - 90)^2
$$

	a_1	a_2	a_3	a_5	a_7	a_8	a_9
β_1	$3{,}906 \cdot 10^{-1}$	$1{,}008 \cdot 10^{-3}$	$1{,}939 \cdot 10^{-3}$	$1{,}341 \cdot 10^{-5}$	$-1{,}841 \cdot 10^{-9}$	$-3{,}002 \cdot 10^{-8}$	$-9{,}124 \cdot 10^{-8}$
β_2	$8{,}202 \cdot 10^{-3}$	$2{,}238 \cdot 10^{-5}$	$2{,}990 \cdot 10^{-5}$	$1{,}754 \cdot 10^{-7}$	$-3{,}910 \cdot 10^{-11}$	$-3{,}923 \cdot 10^{-10}$	$-1{,}784 \cdot 10^{-9}$
β_3	$8{,}085 \cdot 10^{-2}$	$1{,}795 \cdot 10^{-4}$	$2{,}457 \cdot 10^{-4}$	$2{,}023 \cdot 10^{-6}$	$-3{,}273 \cdot 10^{-10}$	$-4{,}266 \cdot 10^{-9}$	$-1{,}872 \cdot 10^{-8}$
β_4	$6{,}971 \cdot 10^{-3}$	$2{,}101 \cdot 10^{-5}$	$3{,}007 \cdot 10^{-5}$	$1{,}680 \cdot 10^{-7}$	$-3{,}810 \cdot 10^{-11}$	$-3{,}625 \cdot 10^{-10}$	$-1{,}374 \cdot 10^{-9}$
β_5	$2{,}159 \cdot 10^{-1}$	$5{,}564 \cdot 10^{-4}$	$1{,}063 \cdot 10^{-3}$	$7{,}222 \cdot 10^{-6}$	$-1{,}017 \cdot 10^{-9}$	$-1{,}602 \cdot 10^{-8}$	$-4{,}832 \cdot 10^{-8}$

Fig. 7